An Improved Algorithm for the Detection of Cirrus Clouds in the Tibetan Plateau Using VIIRS and MODIS Data

L. XIA,*,+ F. ZHAO,# Y. MA,*,@ Z. W. SUN,& X. Y. SHEN,** AND K. B. MAO*,@,++

* National Hulunber Grassland Ecosystem Observation and Research Station, Institute of Agricultural Resources and Regional Planning, Chinese Academy of Agricultural Sciences, Beijing, China
+ Beijing Research Center of Intelligent Equipment for Agriculture, Beijing Academy of Agriculture and Forestry Sciences, Beijing, China
# Key Laboratory of Ecosystem Network Observation and Modeling, Institute of Geographic Sciences and Natural Resources Research, University of Chinese Academy of Science, Beijing, China
@ Chinese Academy of Agricultural Data and Nutrition, Hong Kong, China
& Space Star Technology Co., Ltd., Beijing, China
** Hydrometeorology and Remote Sensing Laboratory, University of Oklahoma, Norman, Oklahoma
++ State Key Laboratory of Remote Sensing Science, Institute of Remote Sensing and Digital Earth Research Institute, and Beijing Normal University, Beijing, China

(Manuscript received 27 March 2015, in final form 12 September 2015)

ABSTRACT

Cirrus clouds play an important role in the global radiation budget balance. However, the existing MODIS and Visible Infrared Imaging Radiometer Suite (VIIRS) cirrus cloud test algorithms struggle to provide accurate cirrus cloud information for the Tibetan Plateau region. In this study, the 1.38-μm cirrus cloud test was improved by adding 11-μm brightness temperature and a multiday average land surface temperature test. An algorithm sensitivity analysis indicated that the proposed algorithm lowered the threshold of the existing 1.38-μm algorithm to 0.005 in the winter and did not produce any observable misclassifications. Compared to the existing 1.38-μm cirrus test algorithm, the accuracy validation indicated that the improved algorithm detected 31.7% more cirrus clouds than the existing VIIRS 1.38-μm cirrus test and yielded 14% fewer misclassifications than the MODIS 1.38-μm cirrus test.

1. Introduction

In recent years, the effects of cirrus clouds on the global energy balance have been studied extensively, and these studies have indicated that the conventional cirrus cloud observational method is not adequate for the global energy balance research (Liou 2005; Sun et al. 2011, 2014). This inadequacy is even more apparent in the Tibetan Plateau region. The high altitude and low vapor content of the Tibetan Plateau region cause numerous difficulties in the existing 1.38-μm cirrus cloud test (Gao et al. 1993; Frey et al. 2008; Hutchison et al. 2012). This test, which is the most effective daytime cirrus cloud detection method for the Moderate Resolution Imaging Spectroradiometer (MODIS) and the Visible Infrared Imaging Radiometer Suite (VIIRS) sensors, detects cirrus clouds more accurately than other methods, such as the 6.7-μm brightness temperature ($BT_{6.7}$) (Soden and Bretherton 1993; Wu et al. 1993), CO_2 slicing (Menzel et al. 2008), and the 11- and 12-μm brightness temperature difference methods (Saunders and Kriebel 1988). In the Tibetan Plateau region, the existing 1.38-μm cirrus cloud test often misclassifies clear skies as cirrus clouds or causes thin cirrus leakage. In this paper, a modification of the MODIS and VIIRS 1.38-μm cirrus test (Frey et al. 2008; Hutchison et al. 2012) that could suppress the surface reflectance of high elevations and improve cirrus cloud detection accuracy in the Tibetan Plateau region was proposed.

2. Improved algorithm

a. Algorithm and thresholds

Since cirrus clouds are usually distributed at high altitudes, their temperatures are very low (Gao et al. 2002; Ackerman et al. 1990). Therefore, a BT_{11} test could

Corresponding author address: K. B. Mao, National Hulunber Grassland Ecosystem Observation and Research Station, Institute of Agricultural Resources and Regional Planning, Chinese Academy of Agricultural Sciences, 12 Zhongguancun South Avenue, Haidian District, Beijing 100081, China.
E-mail: maokebiao@caas.cn

DOI: 10.1175/JTECH-D-15-0063.1

be used to enhance the results of cirrus cloud tests. In general, the BT_{11} obtained by sensors should be $BT_{cir} < BT_{11} < BT_l$, where BT_{cir} is the brightness temperature of a cirrus cloud and BT_l is the brightness temperature of the land surface. The greatest difficulty when using the BT_{11} auxiliary test is obtaining a simple and consistent threshold that is significantly related to BT_l. One possible threshold option is the land surface temperature (LST) values obtained from ground stations. However, the number of ground stations is limited, and LST distributions can vary significantly among different regions. Thus, the choice of LST data obtained from the ground stations will affect the accuracy of a cirrus cloud test. In this study, a multiday average land surface temperature from MODIS products was used as the threshold in this study.

Figure 1 is the MODIS LST data (Wan 2014) of the Tibetan Plateau for January and July of 2013, including the daily average, 8-day average, and monthly average. As shown in Fig. 1, the 8-day average and monthly average LST values were significantly related to the daily LST, which means that the 8-day average or monthly average LST can, in principle, be used as the thresholds for cirrus detections over the Tibetan Plateau. However, it is found that the present 8-day MODIS operational LST data product can still be contaminated by clouds. Therefore, the monthly averages are selected as the thresholds for this proposed cirrus detection algorithm over Tibet.

As mentioned above, when cirrus exists, the BT_{11} obtained by sensors should be $BT_{cir} < BT_{11} < BT_l$. If we used the monthly mean LST to replace BT_l, we have $BT_{11} < T_{LST}$. However, monthly mean LST cannot be used directly as the threshold, because it is not completely equal to BT_{11} for every day in a month (Xia et al. 2014). Therefore, it should be adjusted before being used. In this study, we used Δt to correct for the difference between BT_{11} and LST, so the $BT_{11} < BT_l$ can be presented as $BT_{11} < T_{LST} + \Delta t$. Combining the current 1.38-μm cirrus test and $BT_{11} < T_{LST} + \Delta t$, the improved cirrus algorithm is as follows:

$$\begin{cases} R_{1.38} > R_t \\ BT_{11} < T_{LST} + \Delta t \end{cases}. \quad (1)$$

In this equation $R_{1.38}$ represents the 1.38-μm channel reflective value obtained by the sensor, R_t represents the threshold of the reflectance test, T_{LST} represents the LST obtained from the MODIS/VIIRS monthly average product, and Δt represents the temperature correction value. In this study, by analyzing more than 100 VIIRS granules over the Tibetan Plateau from 2013 to 2014, we obtained that the value of Δt was 10 in the winter and 8 in the summer, and that R_t was equal to 0.008 for every season.

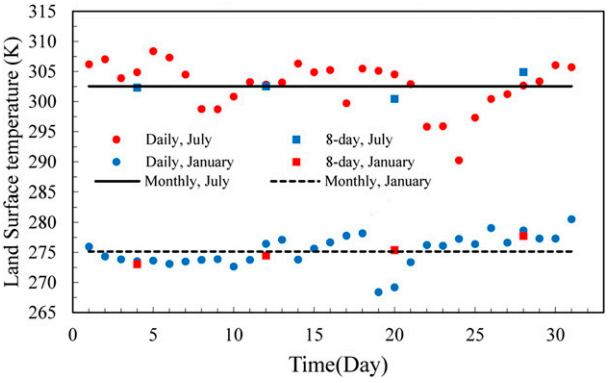

FIG. 1. Daily average, 8-day average, and monthly average LST of the Tibetan Plateau in January and July of 2013.

b. *Threshold sensitivity analysis*

Since BT_{11} was used for additional testing, the number of potential misidentifications increased. A critical threshold sensitivity analysis of the potential misidentifications was conducted.

Figure 2 shows the sensitivity analysis of the VIIRS data for different test thresholds (VIIRS swath data acquired at 0633 UTC 9 January 2013). Figure 2 shows bare land and a frozen lake, with cloud layers primarily distributed in the top-left portion of the image. The 1.38-μm (VIIRS band M9) reflectance value of the lake was approximately 0.04, the ground surface reflectance value was approximately 0.1, and the cloud layer reflectance value ranged from approximately 0.1 to 0.4.

As shown in Fig. 2, the accuracy of the new cirrus cloud test was relatively high over the lake and bare land for different threshold values. The bare land and frozen lake did not appear to be misclassified. Although the reflectance value of the bare land was approximately 0.1, the proposed test did not misinterpret the bare land as cirrus clouds when $R_t = 0.01$, for the reason that Δt can prevent the misclassification of clear surface pixels as thin cirrus pixels, as shown in Figs. 2g,j.

The proposed test, with the different R_t and $|\Delta t|$ values shown in Figs. 2g–m), yielded some misclassifications at the junctions of the lake and land. This was primarily due to the utilization of the 5-km resolution MOD11C3 product. After sampling the 5-km LST data to 750 m (the resolution of the VIIRS M band), the brightness temperatures of these junctions were composed of the brightness temperatures of the lake and the bare land. This indicated that the resampled bare land could have had a lower LST value than the actual LST, resulting in misclassifications when compared to the VIIRS M15 brightness temperature. This would also explain why almost no false alarms occurred at the center of the lake. After increasing the resolution of T_{LST} to 1 km, the false alarms decreased significantly

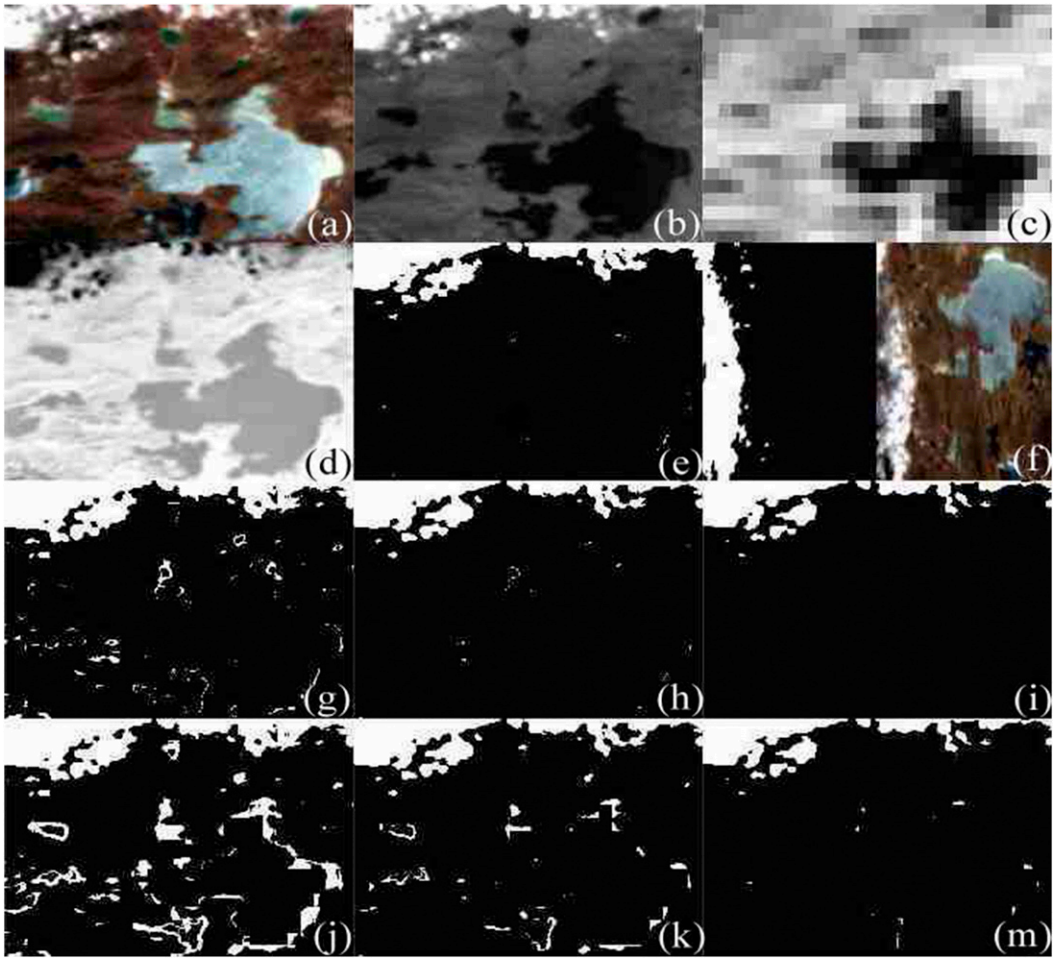

FIG. 2. Sensitivity analysis of the proposed test for different VIIRS data test thresholds (VIIRS swath data acquired at 0633 UTC 9 Jan 2013): (a) triband true color composite image of the VIIRS M5, M4, and M3; (b) VIIRS M9 band reflectance value; (c) LST product obtained from the *Aqua* MODIS monthly MOD11C3 (5-km resolution); (d) VIIRS M15 brightness temperature; (e) results of the proposed cirrus cloud test using VIIRS data and the test thresholds R_t = 0.04 and $\Delta t = -8$, and T_{LST} obtained from the *Aqua* MODIS 8-day MYD11A2 LST product (1-km resolution); (f) results of the proposed cirrus cloud test using (left) MODIS data and (right) MODIS 1, 4, 3 triband true color composite image; (g)–(i) results of the proposed cirrus cloud test for $R_t = 0.01$ and $\Delta t = -5, -8$, and -11, respectively; (j)–(m) results of the proposed cirrus cloud test for $R_t = 0.005$ and $\Delta t = -5, -8$, and -11, respectively.

compared to the cirrus cloud test results (Fig. 2e). When T_{LST} and the 11-μm brightness temperature had the same resolution, the proposed test with the MODIS data did not yield any misclassifications at the junctions of the lake and bare land. Therefore, the misclassifications at the junctions were primarily due to the relatively low resolution of the input T_{LST} data, which could be prevented by increasing the resolution of the LST data.

3. Validation

a. CALIOP data and processing

Cloud–Aerosol Lidar with Orthogonal Polarization (CALIOP) provides the detailed cloud and aerosol profile data that are often used to evaluate the accuracy of cloud-related property retrieval (Holz et al. 2008; Jethva et al. 2014). In this study, CALIOP level 2, 5-km vertical feature mask (VFM, product version 3.30) data were used to validate the accuracy of the enhanced algorithm.

The VFM data product describes the vertical and horizontal distribution of the cloud and aerosol profiles observed by the CALIOP, and the vertical and horizontal resolution of the VFM data varies as a function of altitude above mean sea level (Hunt et al. 2009). Usually, each profile was divided into 545 layers, and every layer was characterized by a single 16-bit integer, with the various bits in the integer representing flags that describe the aerosol and cloud information within the

TABLE 1. Precision analysis of the proposed and existing test results. New indicates the new test presented in the study. Existing indicates the existing VIIRS/MODIS cirrus test. FA is an abbreviation for false alarm (misclassification). NC indicates the pixel number of cirrus clouds detected by the test. Rate of leakage (FA, NC) is the ratio of the number of leakage pixels (FA, NC) to the number of total pixels.

		Pixel No.				Rate (%)		
Sensor	Algorithm	Leakage	FA	NC	Total	Leakage	FA	NC
VIIRS	New	6353	593	13 021	24 952	25.5	2.4	52.2
	Existing	14 261	566	5113	24 952	57.2	2.3	20.5
MODIS	New	15 887	1166	19 711	51 398	30.9	2.3	38.3
	Existing	11 365	8358	24 233	51 398	22.1	16.3	47.1

layer; for example, bits 1–3 specify feature type (cloud, aerosol, surface, etc.) and bits 10–12 specify feature type (cloud, aerosol, etc.).

In this study, the definition of the cirrus cloud is the same as the cirrus cloud detected by CALIOP, which is defined by the International Satellite Cloud Climatology Project (ISCCP) (Rossow and Schiffer 1991). The rule of filtration cirrus cloud in the VFM flags is the value of bits 1–3 equals 2 (cloud) and the value of bits 10–12 equals 6 (cirrus, transparent); for noncirrus cloud the rule is the value of bits 1–3 equals 2 (cloud) and the value of bits 10–12 is not equal to 6.

Besides, considering the existence of multilayer cloud means noncirrus cloud may locate higher than cirrus. In this situation, the VFM data will indicate the existence of cirrus thin, but the VIIRS and MODIS cannot sense the information below the cloud top and this will lead to error. As a result, only the top-layer cloud information of the VFM data was cirrus and the continuous distribution of the cirrus layers was no less than 5; the pixel of this VFM data would be recognized as cirrus.

b. Results

The VIIRS and MODIS swaths of the Tibetan Plateau region from 1 January 2014 to 31 January 2015 were selected to validate the accuracy of the new test. The method used to obtain the matching datasets of CALIOP, MODIS, and VIIRS for the same geographical position was proposed by Nagle and Holz (2009). The imaging interval between CALIOP and MODIS was within 15 min—the same as that between CALIOP and VIIRS.

Table 1 displays the results of the proposed test and the existing MODIS and VIIRS 1.38-μm cirrus cloud test. The existing MODIS cirrus cloud tests were not conducted in the Tibet Plateau, and the test threshold used in the analysis was 0.04. The false alarm (FA; misclassification) column means misclassification of CALIOP clear-sky scenes and CALIOP observed other cloud types as cirrus cloud, and the NC column indicates the pixel number of cirrus clouds detected by the test.

The thresholds used in the VIIRS cloud mask (VCM) 1.38-μm cirrus algorithm (Hutchison et al. 2012; Baker 2014) are functions of the total precipitable water (TPW). If the TPW is less than the minimum TPW, then the cirrus test is not performed. In the Tibetan Plateau region, the TPW during the winter is often too low to perform the VIIRS 1.38-μm cirrus test with reasonable thresholds, leading to significant leakage. However, the proposed test functioned well under these conditions, as shown in Table 1.

The MODIS cirrus test uses constant thresholds for different land types (Frey et al. 2008). As shown in Table 1, the existing MODIS test, with a constant test threshold of 0.04, yielded a low leakage rate but a high misclassification rate of 16.3%. Compared to the existing VIIRS and MODIS tests, the proposed test detected 31.7% more cirrus clouds than the VIIRS test and yielded 14% fewer false alarms than the constant MODIS test. In fact, because of the LST data used in the test with a resolution of only 5 km, the number of misclassifications yielded by the VIIRS test slightly increased.

The monthly leakage and false alarms rates of the existing VIIRS test and proposed test is shown in Fig. 3. As shown in this figure, the existing VIIRS test performed better in the summer than in the winter. This indicated that the existing VIIRS cirrus test was significantly dependent on the TPW. If the amount of TPW was not sufficient, the test used higher thresholds and

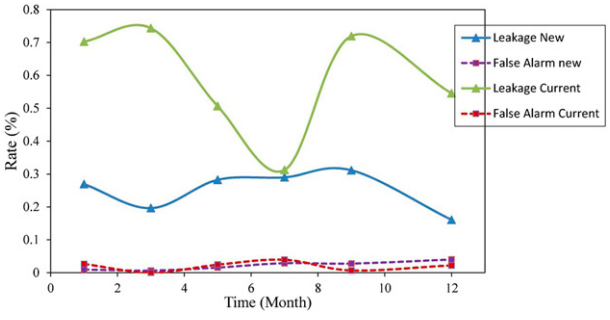

FIG. 3. Leakage and false alarm rates of the existing VIIRS and new tests.

yielded inaccurate results. In contrast, the proposed test performed well even for low TPW values.

4. Conclusions

To detect an increased number of cirrus clouds in the Tibetan Plateau region, an 11-μm brightness temperature was used to enhance the 1.38-μm cirrus test; multiday LST data were used as the brightness temperature test thresholds.

Although the existing VIIRS cirrus cloud test algorithm is very effective when there is a suitable amount of TPW, some areas with low vapor content during the winter, such as the Tibetan Plateau region, might not meet this condition. The proposed test detected 31.7% more cirrus clouds than the existing VIIRS test without any obvious increase in misclassifications. In addition, the proposed test yielded 14% fewer misclassifications than the MODIS test. However, since the proposed test was dependent on the LST, it might not perform adequately for LST values less than 260 K.

Acknowledgments. The authors would like to thank the Goddard Space Flight Center for providing the MODIS and VIIRS data, and Dr. F. W. Nagle from the University of Wisconsin–Madison for providing a procedure to match up the MODIS, VIIRS, and CALIOP data. This work was supported by the National Natural Science Foundation of China (41571427 and 41440047), the Open Fund of the State Key Laboratory of Remote Sensing Science (Grant OFSLRSS 201515), and the National Non-Profit Institute Research Grant of CAAS (IARRP-2015-26).

REFERENCES

Ackerman, S. A., W. L. Smith, H. E. Revercomb, and J. D. Spinhirne, 1990: The 27–28 October 1986 FIRE IFO cirrus case study: Spectral properties of cirrus clouds in the 8-12 μm window. *Mon. Wea. Rev.*, **118**, 2377–2388, doi:10.1175/1520-0493(1990)118<2377:TOFICC>2.0.CO;2.

Baker, N., 2014: Joint Polar Satellite System (JPSS) VIIRS cloud mask (VCM). Algorithm Theoretical Basis Doc. Revision D, 117 pp. [Available online at http://npp.gsfc.nasa.gov/sciencedocs/2015-06/474-00033_ATBD-VIIRS-Cloud-Mask_E.pdf.]

Frey, R. A., S. A. Ackerman, Y. Liu, K. I. Strabala, H. Zhang, J. R. Key, and X. Wang, 2008: Cloud detection with MODIS. Part I: Improvements in the MODIS cloud mask for collection 5. *J. Atmos. Oceanic Technol.*, **25**, 1057–1072, doi:10.1175/2008JTECHA1052.1.

Gao, B.-C., A. F. H. Goetz, and W. J. Wiscombe, 1993: Cirrus cloud detection from airborne imaging spectrometer data using the 1.38 μm water vapor band. *Geophys. Res. Lett.*, **20**, 301–304, doi:10.1029/93GL00106.

——, P. Yang, W. Han, R. R. Li, and W. J. Wiscombe, 2002: An algorithm using visible and 1.38-μm channels to retrieve cirrus cloud reflectances from aircraft and satellite data. *IEEE Trans. Geosci. Remote Sens.*, **40**, 1659–1668, doi:10.1109/TGRS.2002.802454.

Holz, R. E., S. A. Ackerman, F. W. Nagle, R. Frey, S. Dutcher, R. E. Kuehn, M. A. Vaughan, and B. Baum, 2008: Global Moderate Resolution Imaging Spectroradiometer (MODIS) cloud detection and height evaluation using CALIOP. *J. Geophys. Res.*, **113**, D00A19, doi:10.1029/2008JD009837.

Hunt, W. H., D. M. Winker, M. A. Vaughan, K. A. Powell, P. L. Lucker, and C. Weimer, 2009: CALIPSO lidar description and performance assessment. *J. Atmos. Oceanic Technol.*, **26**, 1214–1228, doi:10.1175/2009JTECHA1223.1.

Hutchison, K. D., B. D. Iisager, and B. Hauss, 2012: The use of global synthetic data for pre-launch tuning of the VIIRS cloud mask algorithm. *Int. J. Remote Sens.*, **33**, 1400–1423, doi:10.1080/01431161.2011.571299.

Jethva, H., O. Torres, F. Waquet, D. Chand, and Y. Hu, 2014: How do A-train sensors intercompare in the retrieval of above-cloud aerosol optical depth? A case study-based assessment. *Geophys. Res. Lett.*, **41**, 186–192, doi:10.1002/2013GL058405.

Liou, K. N., 2005: Cirrus clouds and climate. *McGraw-Hill Yearbook of Science and Technology 2005.* McGraw Hill Yearbook of Science and Technology Series, McGraw-Hill Professional, 51–53.

Menzel, W. P., and Coauthors, 2008: MODIS global cloud-top pressure and amount estimation: Algorithm description and results. *J. Appl. Meteor. Climatol.*, **47**, 1175–1198, doi:10.1175/2007JAMC1705.1.

Nagle, F. W., and R. E. Holz, 2009: Computationally efficient methods of collocating satellite, aircraft, and ground observations. *J. Atmos. Oceanic Technol.*, **26**, 1585–1595, doi:10.1175/2008JTECHA1189.1.

Rossow, W. B., and R. A. Schiffer, 1991: ISCCP cloud data products. *Bull. Amer. Meteor. Soc.*, **72**, 2–20, doi:10.1175/1520-0477(1991)072<0002:ICDP>2.0.CO;2.

Saunders, R. W., and K. T. Kriebel, 1988: An improved method for detecting clear sky and cloudy radiances from AVHRR data. *Int. J. Remote Sens.*, **9**, 123–150, doi:10.1080/01431168808954841.

Soden, B., and F. P. Bretherton, 1993: Upper tropospheric relative humidity from GOES 6.7 μm channel: Method and climatology for July 1987. *J. Geophys. Res.*, **98**, 16 669–16 688, doi:10.1029/93JD01283.

Sun, W., G. Videen, S. Kato, B. Lin, C. Lukashin, and Y. Hu, 2011: A study of subvisual clouds and their radiation effect with a synergy of CERES, MODIS, CALIPSO, and AIRS data. *J. Geophys. Res.*, **116**, D22207, doi:10.1029/2011JD016422.

——, ——, and M. I. Mishchenko, 2014: Detecting super-thin clouds with polarized sunlight. *Geophys. Res. Lett.*, **41**, 688–693, doi:10.1002/2013GL058840.

Wan, Z., 2014: New refinements and validation of the collection-6 MODIS land-surface temperature/emissivity product. *Remote Sens. Environ.*, **140**, 36–45, doi:10.1016/j.rse.2013.08.027.

Wu, X., J. J. Bates, and S. Singhkhalsa, 1993: A climatology of the water vapor band brightness temperatures for NOAA operational satellites. *J. Climate*, **6**, 1282–1300, doi:10.1175/1520-0442(1993)006<1282:ACOTWV>2.0.CO;2.

Xia, L., K. B. Mao, Y. Ma, F. Zhao, L. Jiang, X. Shen, and Z. Qin, 2014: An algorithm for retrieving land surface temperatures using VIIRS data in combination with multi-sensors. *Sensors*, **14**, 21 385–21 408, doi:10.3390/s141121385.